Supporting Information

Achieving Tunable Ultra-Broadband NIR emission Originate from Two-Site Occupation of Cr^{3+} Ions in $Mg_3Ga_2SnO_8:Cr^{3+}$

Pengcheng Luo[a,b], Dashuai Sun[a,*], Zeyu Lyu[a], Ming-xiang You[a], Zheng Lu[a], Xiaowei Zhang[a], Luhui Zhou[a], and Hongpeng You[a,b,*]

[a] *Key Laboratory of Rare Earths and Institute of Material and Chemistry, Ganjiang Innovation Academy, Chinese Academy of Sciences, Ganzhou 341000, P.R. China.*

[b] *School of Chemistry and Chemical Engineering, Nanchang University, Nanchang 330031, P.R. China.*

Experimental section

Sample synthesis

A series of $Mg_3Ga_2SnO_8:Cr^{3+}$ samples were synthesized via the conventional high-temperature solid-state reaction. The starting ingredients included MgO (99.999%), Ga_2O_3 (99.99%), SnO_2 (99.8%), and Cr_2O_3 (99.99%) were weighed stoichiometrically and mixed thoroughly. The mixtures were then put in corundum crucibles and heated at 1300 °C for 4 h in a muffle furnace. Finally, the samples were furnace-cooled to room temperature and ground into powders for measurements.

Characterizations

XRD results are acquired using Bruker D8 Advance diffractometer with Cu-Kα radiation. Structural characterization and Rietveld refinement were performed utilizing the FullProf software. The diffuse reflection (DR) spectra were measured by a UV-vis-NIR spectroscopy (Shimadzu UV-3600) using $BaSO_4$ as a reference. X-ray photoelectron spectroscopy (XPS) data were acquired utilizing a Thermo Scientific K-α instrument and a monochromatic Al-Ka line source. The elemental distribution and morphologies were observed and analyzed using a scanning electronic microscope (JSM-IT800, JEOL) equipped with an energy-dispersive X-ray spectrometer. The emission and excitation spectra, and luminescent decay curves of samples were collected using a fluorescence spectrophotometer (Edinburgh Instruments, FLS-1000). The quantum efficiency was measured using an Edinburgh Instruments FLS-1000 spectrometer with an optical integrating sphere. The performance results of the NIR pc-LEDs were gathered through the use of an integrating sphere spectroradiometer system (HASS-2000, Everfine).

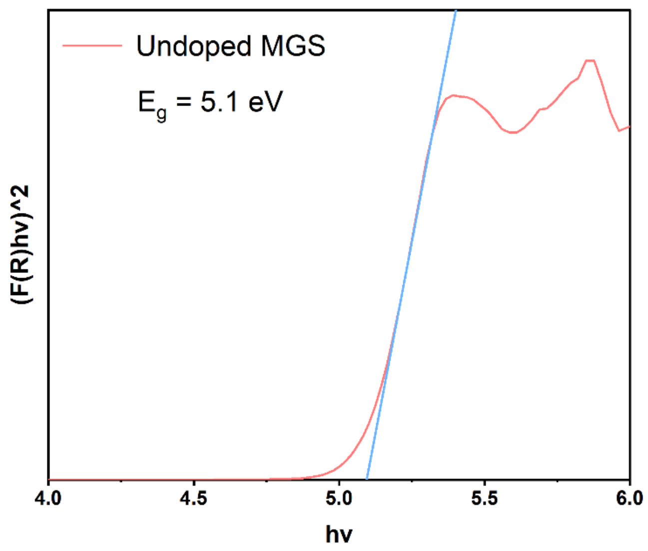

Figure S1 Tucker curve of the undoped MGS.

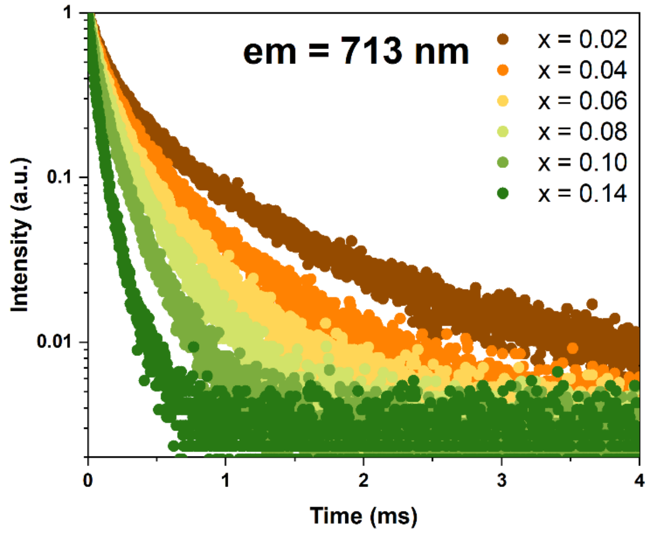

Figure S2 Fluorescence decay curves at 713 nm of MGS:xCr^{3+}.

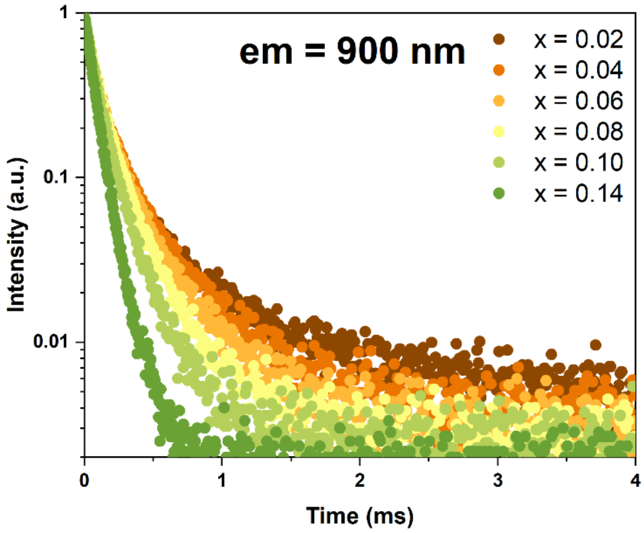

Figure S3 Fluorescence decay curves at 900 nm of MGS:xCr^{3+}.

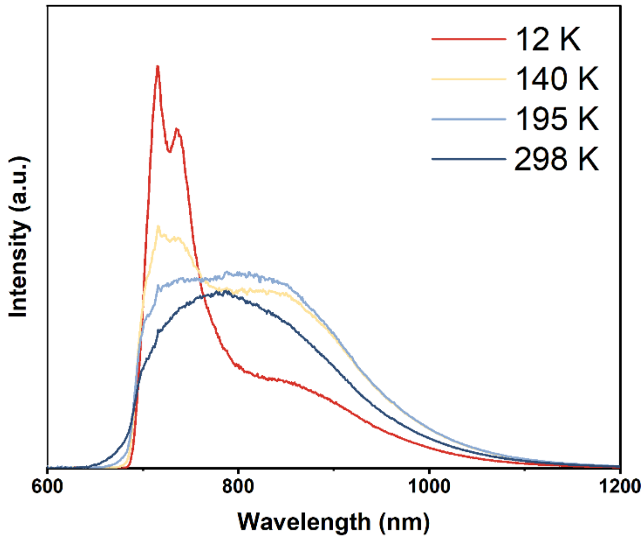

Figure S4 Emission spectra of MGS:0.08Cr^{3+} in different temperature.

Table S1. Refined Structure Parameters of compound MGS:0.08Cr^{3+}.

atom	site	x	y	z	occ.
Mg1	8a	-0.125	-0.125	-0.125	1.000
Mg2	16d	0.500	0.500	0.500	0.250
Sn1	16d	0.500	0.500	0.500	0.230
Ga1	16d	0.500	0.500	0.500	0.480
Cr1	16d	0.500	0.500	0.500	0.040
O1	32e	0.256	0.256	0.256	1.000
Space group: Fd-3m; a = 8.447 Å, b = 8.447 Å, c = 8.447 Å, V = 602.805 $Å^3$; R_{wp} = 9.51%, R_p = 6.69%, χ^2 = 1.55.					

Table S2. PL lifetime at 713 and 900 nm of Cr^{3+} ions in MGS:xCr^{3+}.

Concentration	Photoluminescent lifetime at 713 nm (ms)	Photoluminescent lifetime at 900 nm (ms)
0.02	0.3683	0.1757
0.04	0.2576	0.1675
0.06	0.2081	0.1566
0.08	0.1711	0.1456
0.10	0.1335	0.1280
0.14	0.0852	0.0895

Table S3. Comparison of the FWHM and thermal stability of the phosphors.

Phosphor	FWHM (nm)	Thermal stability (%)	Ref.
$Mg_3Ga_2SnO_8:Cr^{3+}$	212	50.0	This work
$Ga_4GeO_8:Cr^{3+}$	215	56.0	1
$LaScB_4O_{12}:Cr^{3+}$	209	30.2	2
$NaScP_2O_7:Cr^{3+}$	200	53.8	3
$Sr_6Sc_2Al_4O_{15}:Cr^{3+}$	241	<14.6%	4
$LiScSnO_4:Cr^{3+}$	227	~30%	5
$LiInF_4:Cr^{3+}$	210	<27%	6
$LiIn_2SbO_6:Cr^{3+}$	225	<10%	7

Table S4. Photoelectric conversion efficiency and output power of NIR pc-LED1.

Current (mA)	NIR efficiency (%)	Total efficiency (%)	NIR output power (mW)	Total output power (mW)
10	14.43775	16.0345	3.8094	4.2299
20	13.11161	14.5858	7.1356	7.9373
40	11.29572	12.66273	12.632	14.162
60	10.08146	11.25778	17.327	19.351
80	9.10842	10.16944	21.331	23.827
100	8.30926	9.26715	24.74	27.605
120	7.62432	8.46071	27.706	30.753
140	6.97469	7.78633	30.063	33.57
160	6.38323	7.13971	31.92	35.69
180	5.82843	6.51321	33.278	37.195
200	5.28463	5.93256	34.014	38.195

Table S5. Photoelectric conversion efficiency and output power of NIR pc-LED2.

Current (mA)	NIR Efficiency (%)	Total Efficiency (%)	NIR output power (mW)	Total output power (mW)
10	16.38476	17.70205	4.3223	4.6675
20	15.06228	16.65417	8.1981	9.0642
40	13.34584	14.67661	14.938	16.429
60	11.72031	13.01231	20.173	22.402
80	10.45032	11.54747	24.529	27.11
100	9.31931	10.33762	27.82	30.864
120	8.3251	9.27684	30.34	33.815
140	7.39685	8.28624	31.981	35.838
160	6.56309	7.37983	32.927	37.015
180	5.81129	6.53868	33.29	37.466
200	5.10854	5.77975	32.993	37.336

Reference

[1] L. Yao, Q. Shao, M. Shi, T. Shang, Y. Dong, C. Liang, J. He, J. Jiang, Efficient Ultra-Broadband $Ga_4GeO_8:Cr^{3+}$ Phosphors with Tunable Peak Wavelengths from 835 to 980 nm for NIR pc-LED Application, Adv. Opt. Mater. 2021, 2102229.

[2] T. Gao, W. Zhuang, R. Liu, Y. Liu, C. Yan, X. Chen, Design of a Broadband NIR Phosphor for Security-Monitoring LEDs: Tunable Photoluminescence Properties and Enhanced Thermal Stability, Cryst. Growth Des. 2020, 20, 3851-3860.

[3] X. Zhang, P. Dai, D. Wen, Ultra-broadband of up to 200 nm near-infrared phosphors based on one-site occupation strategy for multipurpose applications in light-emitting diodes, Ceram. Int. 2023, 49, 4881-4888.

[4] J. Wang, X. Wang, C. Zhang, X. Zhang, T. Zhou, R.-J. Xie, Broadband emitting phosphor $Sr_6Sc_2Al_4O_{15}:Cr^{3+}$ for near-infrared LEDs, J. Mater. Chem. C. 2023, 11, 9030-9036.

[5] S. Wang, R. Pang, X. Chen, T. Tan, Q. Wang, C. Li, S. Zhang, T. Tan, H. You, H. Zhang, An ultra broadband NIR phosphor $LiScSnO_4:Cr^{3+}$ with emission wavelength peaking at 900 nm for component analysis, Ceram. Int. 2024, 50,1452-1460.

[6] L. Song, S. Liang, W. Nie, X. He, J. Hu, F. Lin, H. Zhu, Ultra-broad Near-Infrared Emitting Phosphor $LiInF_4:Cr^{3+}$ with Extremely Weak Crystal Field, Inorg Chem. 2023, 62, 11112-11120.

[7] D. Liu, G. Li, P. Dang, Q. Zhang, Y. Wei, H. Lian, M. Shang, C.C. Lin, J. Lin, Simultaneous Broadening and Enhancement of Cr^{3+} Photoluminescence in $LiIn_2SbO_6$ by Chemical Unit Cosubstitution: Night-Vision and Near-Infrared Spectroscopy Detection Applications, Angew Chem Int Ed Engl. 2021, 60, 14644-14649.